Available online at www.sciencedirect.com

ScienceDirect

Advances in Climate Change Research xx (2016) 1−9

www.keaipublishing.com/en/journals/accr/

Effects of climate changes on dust aerosol over East Asia from RegCM3

ZHANG Dong-Feng[a], GAO Xue-Jie[b,*], Ashraf ZAKEY[c], Filippo GIORGI[d]

[a] *Shanxi Climate Center, Taiyuan 030006, China*
[b] *Climate Change Research Center, Institute of Atmospheric Physics, Chinese Academy of Sciences, Beijing 100029, China*
[c] *Egyptian Meteorological Authority, Cairo 11784, Egypt*
[d] *The Abdus Salam International Centre for Theoretical Physics, Trieste 34100, Italy*

Received 1 February 2016; revised 13 May 2016; accepted 18 July 2016

Abstract

In order to understand impacts of global warming on dust aerosol over East Asia, a regional climate model (RegCM3) coupled with a dust model is employed to simulate the present (1991−2000, following the observed concentration of the greenhouse gases) and future (2091−2100, following the A1B scenario) dust aerosol. Three experiments are performed over East Asia at a horizontal resolution of 50 km, driven by the outputs from a global model of the Model for Interdisciplinary Research on Climate (MIROC3.2_hires), two without (Exp.1 for the present and Exp.2 for the future) and one with (Exp.3 for the future) the radiative effects of dust aerosols. Effects of climate changes on dust aerosols and the feedback of radiative effects in the future are investigated by comparing differences of Exp.2 and Exp.1, Exp.3 and Exp.2, respectively. Results show that global warming will lead to the increases of dust emissions and column burden by 2% and 14% over East Asia, characterized by the increase in December−January−February−March (DJFM) and the decrease in April−May (AM). Similar variations are also seen in the projected frequencies of high dust emission events, showing an advanced active season of dust in the future. The net top-of-atmosphere (TOA) radiative forcing is positive over the desert source regions and negative over downwind regions, while the surface radiative forcing is negative over the domain, which will lead to a reduction of dust emissions and column burden.

Keywords: Dust aerosol; Climate changes; RegCM3; Numerical simulations

1. Introduction

As a main component of tropospheric aerosols, dust aerosol is entrained into the atmosphere with the amount of 1000−3000 Tg per year, which accounts for about half of the total tropospheric aerosols (Cakmur et al., 2006). In East Asia, dust aerosol from the nature source of Gobi desert and northwestern China alone contributes the amount of 800 Tg per year (Zhang et al., 1997). Compared to other source regions, East Asian dust is more likely to be transported to wider regions due to its unique geographical location under the proper weather conditions (Jiang and Chen, 2008). It affects the climate, environment and ecology of downwind areas by modifying the radiation budget through absorption and scattering of incoming solar radiation and outgoing long-wave radiation (Shi and Zhao, 2003).

The study of dust aerosol can be dated back to the 1920s (Hankin, 1921) with the focus mainly on the characteristic of strong dust events, including temporal and spatial distributions, mechanisms and structures, etc. After 1970s, comprehensive monitoring of dust aerosol becomes active with the development of satellite retrievals and ground observation network (Shenk and Curian, 1974). Subsequently, climatic

* Corresponding author.
E-mail address: gaoxuejie@mail.iap.ac.cn (GAO X.-J.).

Peer review under responsibility of National Climate Center (China Meteorological Administration).

Production and Hosting by Elsevier on behalf of KeAi

http://dx.doi.org/10.1016/j.accre.2016.07.001

responses caused by dust aerosol are quite well documented through the analysis of disturbed radiation balance between surface and atmosphere (Zhang and Christopher, 2003). Studies for global and regional dust become the hot spots in recent years (Westphal et al., 1988; Zakey et al., 2006; Zhang et al., 2009; Fiedler et al., 2015).

Most of studies mentioned above discussed the present dust, but the speculation about the possible changes of dust under global warming have been rarely described (Mahowald and Luo, 2003; Tegen et al., 2004; Mahowald et al., 2006; Liu et al., 2014) and almost inferred from global models with coarse resolutions (Mahowald and Luo, 2003; Tegen et al., 2004; Mahowald et al., 2006). On the one hand, weakened latitudinal temperature gradients due to a larger warming in high latitudes than in tropics and subtropics are likely to result in a less windy and less dusty future in coming decades to centuries; on the other hand, increased evaporation and decreased soil moisture induced by the warming are conducive to an intensification of dusty cycle. Also the change of the precipitation, earlier melt of snow and radiative forcing feedback of dust altogether may cause a shift in dust event frequency, intensity and high-incidence season. To understand the combined effects of the aforementioned elements, numerical models and their simulations are needed.

In the present study, the effects of global warming on the dust aerosol over East Asia are discussed by using a regional climate model (RegCM3) coupled with a desert dust module (Zakey et al., 2006; Solmon et al., 2006; Pal et al., 2007). The model and experiment design are described in Section 2, while simulated present dust and its future change are presented in Section 3. Finally, a brief conclusion and discussion is summarized in Section 4.

2. Model, experiment design and data

The model employed in the study is the Regional Climate Model version 3 (RegCM3) developed at the Abdus Salam International Centre for Theoretical Physics (ICTP) (Pal et al., 2007). The solar (SW) and atmospheric (LW) radiation schemes are described in Kiehl et al. (1996). Land surface processes are represented via the Biosphere-Atmosphere Transfer Scheme (BATS1e) (Dickinson et al., 1993), with the prescribed surface land use type in each model grid. Planetary boundary layer computations employ the non-local formulation of Holtslag et al. (1990). The mass flux scheme of Grell (1993) is used to describe convective precipitation and the sub-grid explicit moisture scheme of Pal et al. (2000) is used to describe non-convective precipitation.

The coupled dust module consists of the processes of dust emissions, transport, deposition of four particle size-bins from 0.01 to 20.0 μm (0.01–1.0 μm, 1.0–2.5 μm, 2.5–5.0 μm and 5.0–20.0 μm), and also takes accounts for optical properties and radiation effects of particle (Zakey et al., 2006). The dust emission scheme is based on Marticorena and Bergametti (1995) and Alfaro and Gomes (2001). Transport processes are described by the tracer transport equation of Solmon et al. (2006) and Zakey et al. (2006). The dry and wet deposition terms are treated following Zakey et al. (2006) and Giorgi (1986, 1989), respectively. The refractive indices of dust aerosols for the relevant SW spectral windows are taken from the Optical Properties of Aerosols and Clouds (OPAC) database (Hess et al., 1998), the dust SW radiative effect is calculated using asymmetry factor, single scattering albedo, and mass extinction coefficient obtained from Mie (1908) calculations. In this study, the amount of dust emissions are decided by soil texture type, soil water content, surface roughness, snow cover and 10 m wind speed, etc. Taking into account the climate background of East Asia, here dust is only emitted from the model grids with land use type of desert or semi-desert and with snow cover of less than 1 mm.

Three experiments were conducted in this study, and each was run for 10 years. The first one (Exp.1) simulates the present (1991–2000) dust, and does not include the radiative forcing; the other two simulate the future (2091–2100) dust under the Special Report on Emissions Scenarios (SRES) A1B scenario (Nakicenovic et al., 2000), one without (Exp.2) and one with (Exp.3) the radiative forcing. The differences between Exp.2 and Exp.1 are considered as the effect of climate change on dust, while the differences between Exp.3 and Exp.2 are regarded as the feedback of dust radiative forcing in the future.

Central point of the model is set at 36°N, 105°E, with 109 grids in the north–south direction and 160 grids in the west-east direction. The model domain encompasses the whole continental China and adjacent areas (Fig. 1) at a horizontal grid spacing of 50 km. It includes the primary dust producing regions in East Asia. The model is run at its standard configuration of 18 vertical sigma layers with model top at 10 hPa.

Initial and lateral boundary conditions are obtained from outputs of the 20th Century Climate in Coupled Models (20C3M) and SRES A1B simulations in the Coupled Model Inter-comparison Project Phase 3 (CMIP3) model of MIROC3.2_hires. This driven model has the highest horizontal resolution of T106 (~ 125 km) in the CMIP3 models and good performance over East Asia (Lucarini et al., 2007; Xu, 2010).

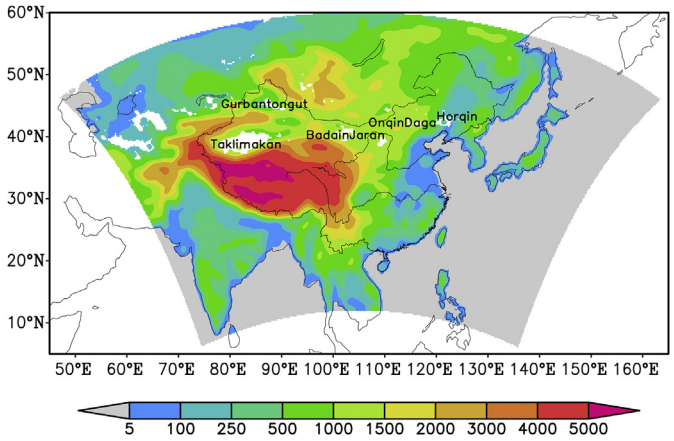

Fig. 1. Model domain and topography (unit: m). Also shown the source regions of dust (white color).

Please cite this article in press as: ZHANG, D.-F., et al., Effects of climate changes on dust aerosol over East Asia from RegCM3, Advances in Climate Change Research (2016), http://dx.doi.org/10.1016/j.accre.2016.07.001

Land use types are based on observed data within China (Liu et al., 2003) and the Global Land Cover Characteristics (GLCC) data developed by the United States Geological Survey (USGS) outside China (Loveland et al., 2000). Soil texture data are based on the United States Department of Agriculture texture classification (USDA, 1999), with some modifications in Northeast China for extra dust sources (Onqin Daga and Horqin) following Shao and Dong (2006).

3. Results

3.1. Present dust aerosol

3.1.1. Multi-annual mean dust emissions, column burden and aerosol optical depth (AOD)

Here simulated multi-annual mean dust aerosol emissions, column burden and optical depth from Exp.1 are selected to compare with the frequency of observed severe dust storms in northern China in 1954–2002 (Zhou and Zhang, 2003). More detailed evaluations of model performance can be found in Zhang et al. (2009).

The observation suggests that severe dust storms appear with high spatial discontinuities in 1954–2002. The large number of occurrences exceeding 10 is found in the Taklimakan, Badain Jaran and Onqin Daga, in particular with the maxima of larger than 20 over the southern of Taklimakan desert, where dust aerosol is the most active (Zhou and Zhang, 2003).

The higher multi-annual mean dust emissions centers from Exp.1 within the territory of China located at the Gurbantonggut, Taklimakan, Badain Jaran, Onqin Daga and Horqin. The high emissions of larger than 10,000 mg m^{-2} d^{-1} over the Taklimakan and Badain Jaran and 5000–10,000 mg m^{-2} d^{-1} over other dust sources are shown as mentioned above. Small emissions can be found over other areas with the capabilities of emissions. For example, dust emissions are less than 250 mg m^{-2} d^{-1} in the northern Tibetan Plateau due to the impact of deep snow cover (Fig. 2a).

Simulated distribution of multi-annual mean dust column burden, as a comprehensive production of dust emissions and its vertical transport process, is essentially similar to that of dust emissions. Over the Taklimakan and Badain Jaran, the values of dust column burden are greater than 500 mg m^{-2}, locally up to 1500–2000 mg m^{-2}. Relatively small values of greater than 250 mg m^{-2} are shown over other dust sources. It is noteworthy that an atmospheric dust column burden of larger than 50 mg m^{-2} can be found at 130°E following the path of prevailing winds (Fig. 2c).

Similarly, distributions of multi-annual mean AOD are characterized by the maxima of more than 0.6 over the Taklimakan and the values of 0.2–0.4 over the Badain Jaran (Fig. 2e).

In summary, the simulated spatial patterns of multi-annual dust emissions, column burden and AOD show large agreements to that of the observed severe dust storms in northern China in 1954–2002. The good performances of the model in reproducing the observed dust climatology increases the confidences of the model in the future dust projections.

3.1.2. Monthly mean dust emissions, column burden and the occurrence of dust event with different emission thresholds

Simulated monthly mean dust emissions in the present (Exp.1) and future (Exp.2) over the domain are provided in Table 1. The present-day annual mean emissions are 2919 g m^{-2} d^{-1}, with the peak emissions of 6294 g m^{-2} d^{-1} and 5900 g m^{-2} d^{-1} in April and May, respectively. The lowest emissions can be found in December and January, with values of less than 1000 g m^{-2} d^{-1}. The pronounced temporal discontinuities are shown in monthly dust producing.

In Table 2, the time evolution of monthly mean dust column burden is shown based on simulations of the present (Exp.1) and future (Exp.2). Similar to the results of present dust emissions, present dust column burden shows the maximum in April and May, with values of 1713 g m^{-2} and 1738 g m^{-2}, respectively, and the minima of 371 g m^{-2} and 329 g m^{-2} in December and January. Annual mean dust column burden is 915 g m^{-2}.

In order to understand the intensity of dust activity, the crude dust event counts in simulations are described with three different emission thresholds of 1500, 2500 and 5000 mg m^{-2} d^{-1}. Fig. 3 shows their monthly occurrences in the present (Exp.1) and future (Exp.2). For all thresholds, the highest dust event frequency occurs in April in the present, with the occurrences of 196, 117, and 36 d per 10 years from the lowest thresholds to the highest one. The numbers of total 10-year dust event occurrences are 984, 406, and 97 d for the three thresholds, respectively.

3.2. Future changes of dust aerosol

3.2.1. Multi-annual mean dust emissions, column burden and AOD

In the future, the spatial distributions of dust emissions, column burden and AOD are similar to the present, maximum centers are still located in the Taklimakan and Badain Jaran (figure not shown for brevity).

As shown in Fig. 2b, less dust emissions can be found over main source regions such as the Taklimakan, Badain Jaran, Onqin Daga, Horqin and southern Mongolia in the future (Exp.2–Exp.1). In the meanwhile a widespread increase of dust emissions is shown in northern Tibet Plateau, where there are relative weaker emissions in the present. The pattern of dust column burden changes is not exactly the same as that of dust emissions, characterized by an increase over the most areas of the Taklimakan (Fig. 2d) as a result of enhanced wind speed in the middle and lower troposphere. For example, although the change of wind speed at 10 m is dominated by a weak decrease over the Taklimakan (Fig. 2g), increased wind speeds of 0.25–1.00 m s^{-1} is projected at 700 hPa (Fig. 2h). A consistent change of dust AOD with column burden can be found in Fig. 2f, with increase of AOD in the Taklimakan source and downwind regions.

Please cite this article in press as: ZHANG, D.-F., et al., Effects of climate changes on dust aerosol over East Asia from RegCM3, Advances in Climate Change Research (2016), http://dx.doi.org/10.1016/j.accre.2016.07.001

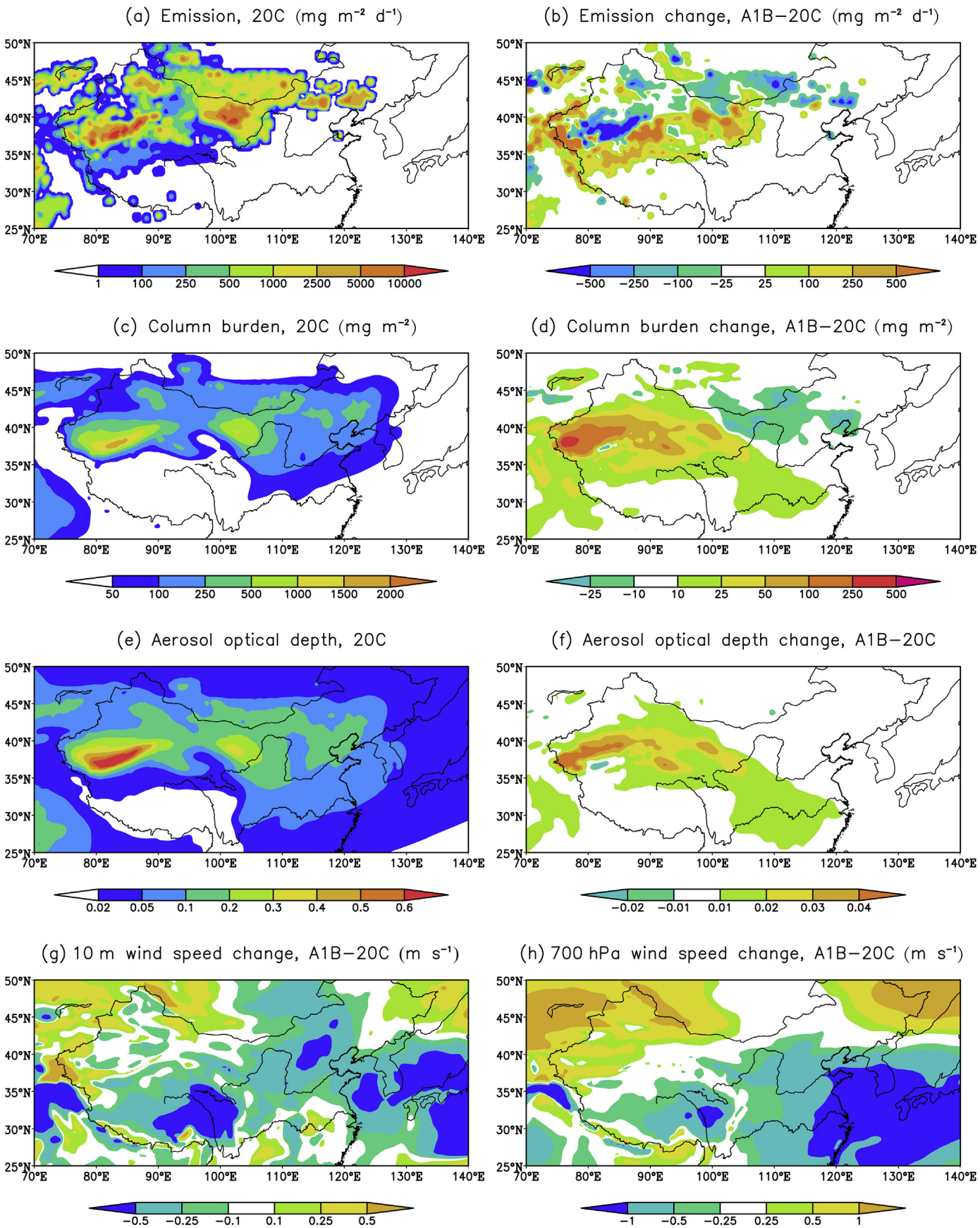

Fig. 2. Simulated multi-annual mean dust emissions (a) and the change (b), column burden (c) and the change (d), aerosol optical depth (e) and the change (f), changes of wind speed at 10 m (g) and 700 hPa (h).

Please cite this article in press as: ZHANG, D.-F., et al., Effects of climate changes on dust aerosol over East Asia from RegCM3, Advances in Climate Change Research (2016), http://dx.doi.org/10.1016/j.accre.2016.07.001

Table 1
Simulated monthly mean dust emissions and the future change (unit: g m^{-2} d^{-1}).

Period and change	Jan	Feb	Mar	Apr	May	Jun	Jul	Aug	Sep	Oct	Nov	Dec	Ave
Present	889	1963	3685	6294	5900	3742	2444	2144	2484	2634	1860	993	2919
Future	1996	3068	5124	4963	5030	3311	2421	1904	1835	2404	1771	2025	2988
Changes	1107	1105	1439	−1331	−870	−431	−23	−240	−649	−230	−89	1032	69
Percent of change (%)	124	56	39	−21	−15	−12	−1	−11	−26	−9	−5	104	2

Table 2
Simulated monthly mean dust column burden and the future change (unit: g m^{-2}).

Period and change	Jan	Feb	Mar	Apr	May	Jun	Jul	Aug	Sep	Oct	Nov	Dec	Ave
Present	329	589	999	1713	1738	1321	890	825	851	800	561	371	915
Future	646	925	1507	1569	1692	1306	1024	890	811	831	640	674	1043
Changes	317	336	508	−144	−46	−15	134	65	−40	31	79	303	128
Percent of change (%)	96	57	51	−8	−3	−1	15	8	−5	4	14	82	14

3.2.2. Monthly mean dust emissions, column burden and the occurrence of dust event with different emission thresholds

Multi-annual mean dust emissions show a slight increase of 2% in the future, with a larger increase of 39%–124% in December–January–February–March (DJFM) and a relatively small decrease of 1%–26% from April to November (Table 1). Note that the largest dust emissions are found in April–May (AM) in the present-day climatology, but the highest emissions occur in March in the future. This is caused by a maximum increase of 1439 g m^{-2} d^{-1} in March and a maximum decrease of 1331 g m^{-2} d^{-1} in April (Table 1). The projected changes of emissions in DJFM and AM are shown in Fig. 4a and c. A robust emissions increase is found over most of domain except the parts of the Taklimakan in DJFM (Fig. 4a). In AM, specific regional changes of emissions mainly associated with topography, dust emissions decrease over areas with lower altitude (including all sources) and increases over areas with high elevation (Fig. 4c).

Multi-annual mean dust column burden increase by 14% in the future, mainly due to its increase in most months, except the slight decrease in April–May–June and September (Table 2). In general, the temporal evolutions of dust column burden change are also consistent with that of dust emissions. A larger increase of 303–508 g m^{-2} is found in DJFM with the maximum value in March, while showing a maximum decrease of −144 g m^{-2} in April. These kinds of time-evolving give rise to a quite similar magnitude of dust column burden in peak seasons of March–April–May (MAM) in the future. The spatial distributions of column burden changes in DJFM and AM show agreements in the sign with emission changes. The relatively uniform increase in DJFM and dominant decrease in AM are found (Fig. 4b and d).

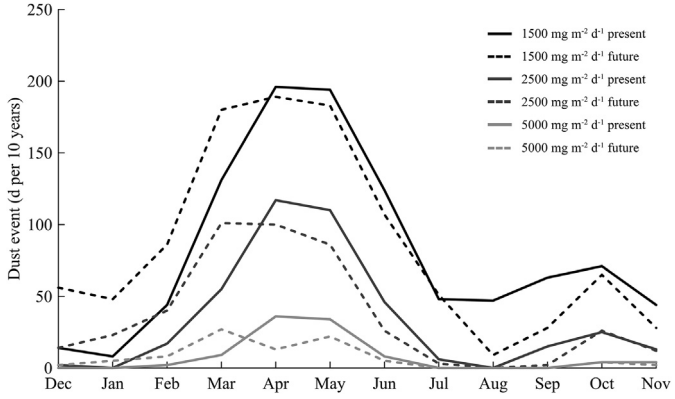

Fig. 3. Number of occurrences of dust event in the present and future, as defined by the emission thresholds 1500, 2500 and 5000 mg m^{-2} d^{-1}.

Numbers of dust events occurrences with the emission thresholds 1500 and 2500 mg m^{-2} d^{-1} increase in DJFM (Fig. 5), with maxima in March compared with that in present-day, and show a mainly reduction from April to November. The numbers of total 10-year occurrences are 1030 and 433 d for above two emission thresholds, showing an increase of 46 and 27 d relative to the present-day (Fig. 3). With 5000 mg m^{-2} d^{-1} as the thresholds, the maxima of increase are still found in March and the highest frequency of occurrences is still in MAM (March–April–May), but it should be noted that the total number of occurrences decreases from 97 d in the present to 88 d in the future due to the pronounced decreases in AM. Results suggest that strongest dust events may decrease in the future.

Changes in monthly mean dust aerosol emissions, column burden and the occurrences of dust event with different emission thresholds show a significant increase in March and reduction in April. All this indicates that there is an advanced active season of dust in the future, and it is likely that there are the same magnitude dust activities in frequency and intensity for the future active season of MAM. Explanation of these changes is that there are declined strong wind events and snow cover areas in the future based upon the simulations. Declined 10 m wind intensities and snow covers over grid boxes with the ability of dust emissions are shown in Fig. 6a–b. Projected number of days with the 10 m wind speeds exceeding 5 m s^{-1} or 6 m s^{-1} decreases in almost months, especially in April and May (Fig. 6a), which lead to the significant decrease of dust emissions. The number of points with the snow cover <1 mm increases in all months, with the larger increase in DJFM (Fig. 6b), which lead to the increased dust activity for these months, although wind speeds at 10 m are weakened at the same time.

Please cite this article in press as: ZHANG, D.-F., et al., Effects of climate changes on dust aerosol over East Asia from RegCM3, Advances in Climate Change Research (2016), http://dx.doi.org/10.1016/j.accre.2016.07.001

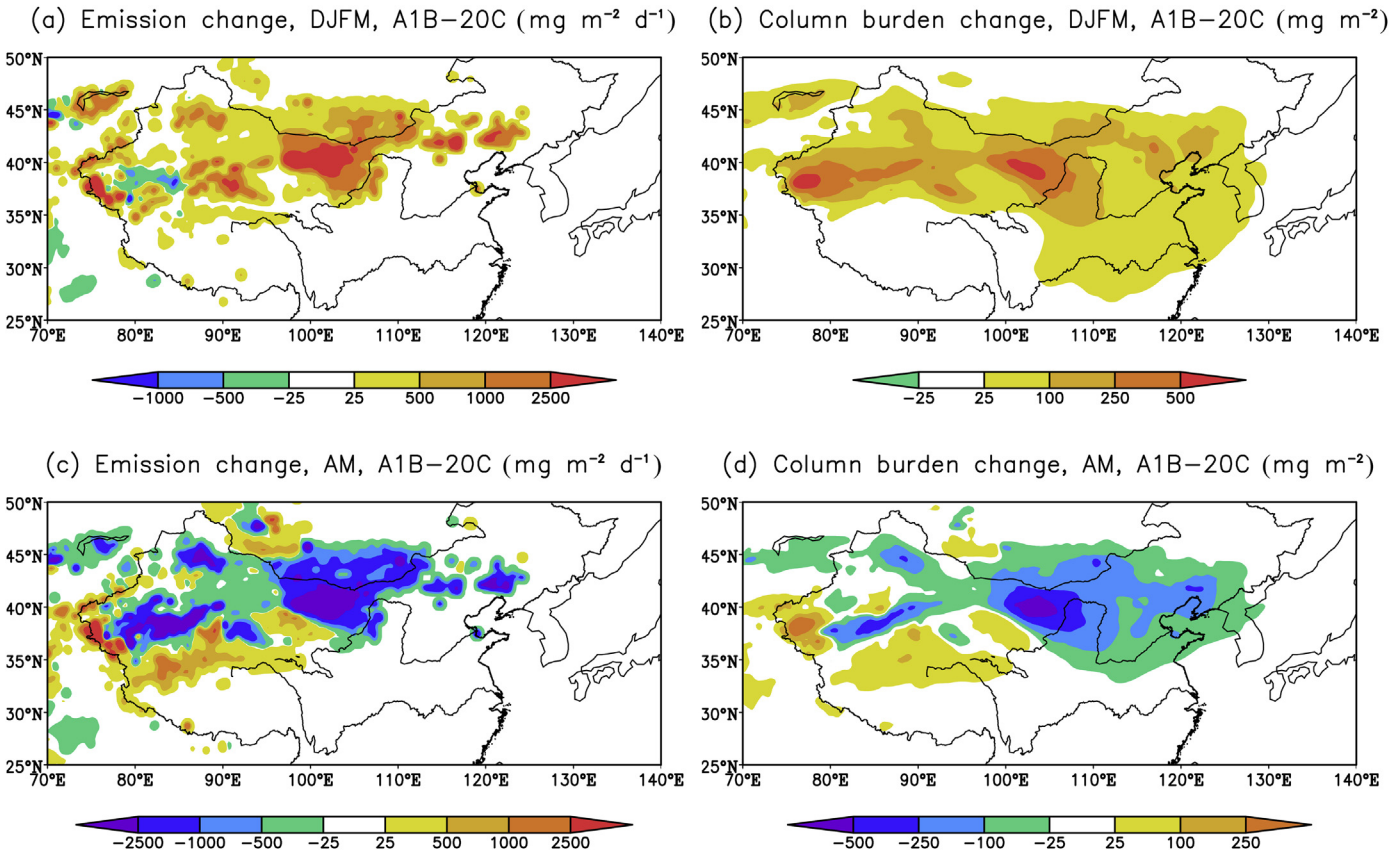

Fig. 4. Simulated emission changes in December–January–February–March (DJFM) (a) and April–May (AM) (c), and column burden changes in DJFM (b) and AM (d).

3.2.3. Dust feedbacks on regional climate

Aerosol-radiation interactions is thought to be important in modifying global and regional climate, though substantial uncertainties remain in assessments due to difficulties in measurement and lack of observations of some relevant parameters. Due to the similar feedback of dust aerosol in the present and future, here only the future radiative forcing at top-of-atmosphere (TOA) and surface, as well as their effects on dust emissions and column burden are briefly analyzed (Exp.3−Exp.2).

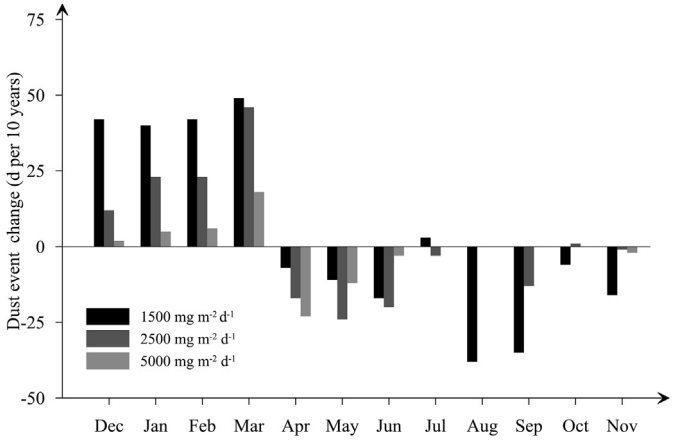

Fig. 5. Change of occurrences of dust event as defined by the emission thresholds 1500, 2500 and 5000 mg m^{-2} d^{-1}.

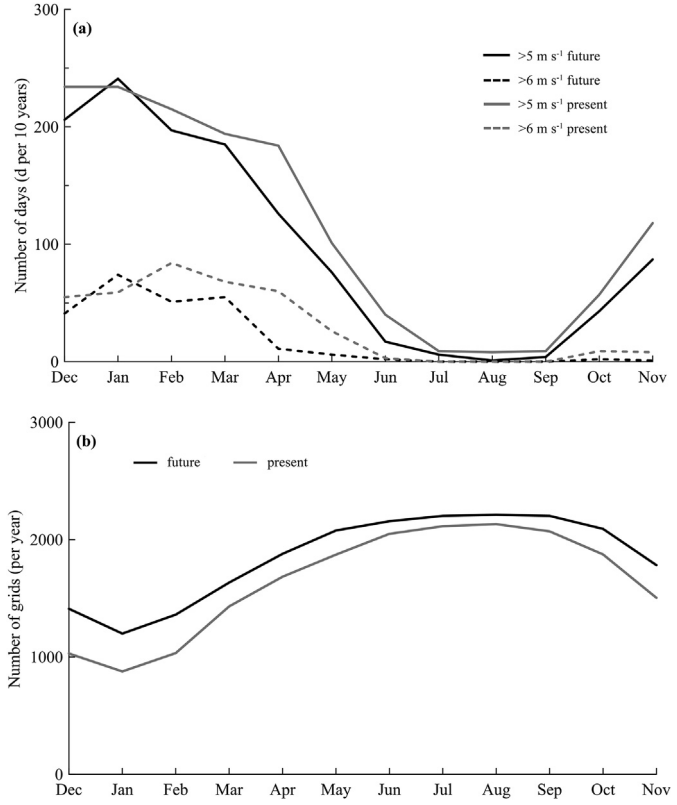

Fig. 6. Number of days (a) with wind speed > 5 m s^{-1} and >6 m s^{-1}, and (b) number of grids with snow cover <1 mm in the present and future.

Please cite this article in press as: ZHANG, D.-F., et al., Effects of climate changes on dust aerosol over East Asia from RegCM3, Advances in Climate Change Research (2016), http://dx.doi.org/10.1016/j.accre.2016.07.001

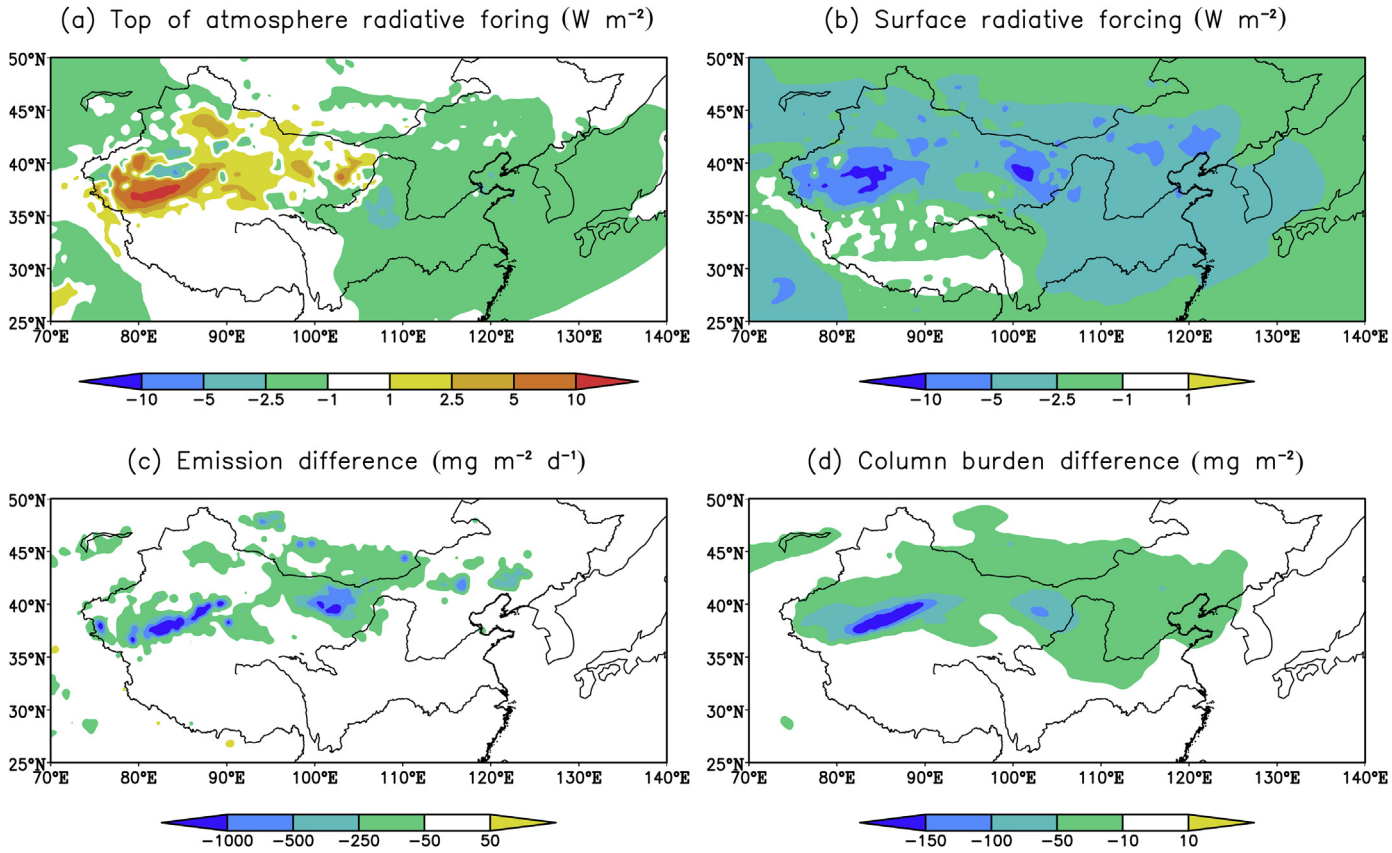

Fig. 7. Top-of-atmosphere (a) and surface (b) radiative forcing and their effects on dust emissions (c) and column burden (d).

Projected radiative forcing and their effects on dust aerosols are given in Fig. 7. The dust exerts a positive TOA forcing over the source regions, with a maximum of exceeding 10 W m^{-2} in the Taklimakan, while a negative TOA forcing dominates the downwind areas (Fig. 7a). Due to scattering and absorption of incoming solar radiation by dust aerosol, a substantial negative surface radiative forcing of up to 10 W m^{-2} over the source regions and 2.5–5.0 W m^{-2} over the downwind regions can be found (Fig. 7b).

Dust negative surface forcing leads to the cooling and the decreased sensible heat fluxes at the surface (Figs omitted), that weakens the turbulence in boundary layer, and then causes the declined surface wind velocity. Finally, there is a reduced dust aerosol emissions locally up to 1000 mg m^{-2} d^{-1} over the Taklimakan and 500 mg m^{-2} d^{-1} over the Badain Jaran, as shown in Fig. 7c.

Dust column burden is declined correspondingly and a decrease of more than 150 mg m^{-2} and 50–100 mg m^{-2} can be found over the Taklimakan and Badain Jaran source areas, respectively. The relatively small decrease of 10–50 mg m^{-2} is shown in the downwind area (Fig. 7d).

4. Summary and discussion

The future dust changes under global warming are examined by using RegCM3 driven by a global model output of MIROC3.2_hires.

Over East Asia, multi-annual mean emissions and column burden of dust aerosol will increase by 2% and 14%, respectively, in 2091–2100 relative to 1991–2000. The annual cycle changes are characterized by an increase in DJFM and a decrease in other months. The former increase is mainly influenced by the less snow cover future, and the latter decrease corresponds to the weakening of 10 m wind speed. Similar changes are shown for the dust event frequencies with different emission thresholds, which may bring an early severe dust event season to a certain extent. It is also noteworthy that the most severe dust event (such as with 5000 mg m^{-2} d^{-1} as the thresholds) will decrease in the future. In addition, the dust exerts a negative surface radiative forcing, a prevailing positive TOA radiative forcing over the source regions and a negative TOA radiative forcing over downwind areas. As a result, the dust radiative forcing induces a negative feedback mechanism on the dust emissions and column burden.

Note that results from this study show some differences with other studies. Such as Mahowald and Luo (2003) suggested that future dust in 2090–2099 may be 20%–60% lower than that in 1990–1999 if the global temperature rise following the A1 scenario. Similar result appears in the global model IS92a scenario simulations by Tegen et al. (2004), dust loadings decrease by 19% in 2070–2080 relative to the period of 1970–1980 over East Asia. However, Liu et al. (2014) investigated the relationship between dust and temperature in the northern Qinghai–Tibetan Plateau with the temperature

Please cite this article in press as: ZHANG, D.-F., et al., Effects of climate changes on dust aerosol over East Asia from RegCM3, Advances in Climate Change Research (2016), http://dx.doi.org/10.1016/j.accre.2016.07.001

reconstructions, suggests that increased temperatures led to strong dust activity, while decreased temperatures resulted in weak dust activity in the northern Qinghai−Tibetan Plateau.

The climate, as the forcing, has a large impact on future dust aerosol. Specific to this study, MIROC3.2_hires projects a warmer and wetter future over East Asia (Xu, 2010; Shi, 2010) as well as a weaker decrease of wind speeds in dust source areas (Jiang et al., 2010), compared to the CMIP3 multi-model ensemble mean under the A1B scenario. Both minor weakening of wind speeds and warmer climate are not conducive to the decrease of dust. Except the forcing data used, inconsistencies between this study and the cited studies may be mainly caused by physical parameterizations used in climate models and coupled dust modules. The mean state and variability of dust are sensitive to the physical parameterizations of models in the land surface processes, the boundary layer scheme, the radiation scheme, the cumulus scheme, dust emissions, transport and deposition, etc. For example, the model applied in our study is limited by 1) missing the re-entrainment process of dust; 2) prescribed land use types and overestimation of snow cover, which lead to the uncertainty of dust projection. Finally, due to limitations of the computer resources, relatively coarse resolution of 50 km and the insufficient simulation length of 10 years are also sources of uncertainties.

Further efforts are needed to reduce uncertainties and improve the understanding of future changes of dust over East Asia and China under the global warming. The efforts include the employment of the more recent global climate models (CMIP5 and the upcoming CMIP6) as the driving fields, simulations using more recent version of RegCM4 and the upcoming RegCM5 with improvement of model physical parameterizations (e.g. introduction of the dust re-entrainment and dynamical vegetation processes, update of the soil freezing module, etc.), and finally, the multi-model ensemble approaches of multiple regional climate models driven by multiple global model under the CORDEX frame (Giorgi et al., 2009).

Acknowledgements

This study was supported by the Special Climate Change Research Program of China Meteorological Administration (No. CCSF201509), and the Special Fund for Meteorological Research in the Public Interest (No. GYHY201306019). Cordial thanks are extended to editors and two anonymous reviewers for their professional comments and suggestions.

References

Alfaro, S.C., Gomes, L., 2001. Modelling mineral aerosol production by wind erosion: emission intensities and aerosol size distributions in source areas. J. Geophys. Res. 106 (D16), 18075−18084.

Cakmur, R.V., Miller, R.L., Perlwitz, J., et al., 2006. Constraining the magnitude of the global dust cycle by minimizing the difference between a model and observations. J. Geophys. Res. 111, D06207. http://dx.doi.org/10.1029/2005JD005791.

Dickinson, R.E., Kennedy, P.J., Henderson-Sellers, A., et al., 1993. Biosphere-Atmosphere Transfer Scheme (BATS) Version1e as Coupled to the NCAR Community Climate Model. NCAR Tech. Note NCAR/TN-387 STR. National Center for Atmospheric Research, Boulder, CO.

Fiedler, S., Knippertz, P., Woodward, S., et al., 2015. A process-based evaluation of dust-emitting winds in the CMIP5 simulation of HadGEM2-ES. Clim. Dyn. http://dx.doi.org/10.1007/s00382-015-2635-9.

Giorgi, F., 1986. A particle dry deposition parameterization scheme for use in tracer transport models. J. Geophys. Res. 91 (D9), 9794−9806.

Giorgi, F., 1989. Two-dimensional simulations of possible mesoscale effects of nuclear war fires: 1. model description. J. Geophys. Res. 94 (D1), 1127−1144.

Giorgi, F., Jones, C., Asrar, G., 2009. Addressing climate information needs at the regional level: the CORDEX framework. WMO Bull. 58 (3), 175−183.

Grell, G., 1993. Prognostic evaluation of assumptions used by cumulus parameterizations. Mon. Weather. Rev. 121, 764−787.

Hankin, E.H., 1921. On dust raising winds and descending currents. India Meteorol. Memoirs 22, 210−223.

Hess, M., Koepke, P., Shult, I., 1998. Optical properties of aerosols and clouds: the software package OPAC. Bull. Am. Metorol. Soc. 79 (5), 831−844.

Holtslag, A.A.M., de Bruijn, E.I.F., Pan, H.-L., 1990. A high resolution air mass transformation model for short-range weather forecasting. Mon. Weather. Rev. 118, 1561−1575.

Jiang, X.-G., Chen, S.-J., 2008. An observational and numerical study on the topography influence on the dust transportation. Acta Meteorol. Sin. 66 (1), 1−12 (in Chinese).

Jiang, Y., Luo, Y., Zhao, Z.-C., 2010. Projection of wind speed changes in China in the 21st century by climate models. Chin. J. Atmos. Sci. 34 (2), 323−336 (in Chinese).

Kiehl, J., Hack, J., Bonan, G., et al., 1996. Description of the NCAR Community Climate Model (CCM3). NCAR Tech. Note NCAR/TN-420 STR. National Center for Atmospheric Research, Boulder, CO.

Liu, X.-Q., Yu, Z.-T., Dong, H.-L., et al., 2014. A less or more dusty future in the northern Qinghai-Tibetan Plateau? Sci. Rep. 4, 6672. http://dx.doi.org/10.1038/srep06672.

Loveland, T.R., Reed, B.C., Brown, J.F., et al., 2000. Development of a global land cover characteristics database and IGBP DISCover from 1-km AVHRR data. Int. J. Remote Sens. 21 (6−7), 1303−1330.

Liu, J.-Y., Liu, M.-L., Zhuang, D.-F., et al., 2003. Study on spatial pattern of land-use change in China during 1995−2000. Sci. China Ser. D Earth Sci. 46 (4), 373−384.

Lucarini, V., Calmanti, S., Dell'Aquila, A., et al., 2007. Intercomparison of the northern hemisphere winter mid-latitude atmospheric variability of the IPCC models. Clim. Dyn. 28, 829−848.

Mahowald, N.M., Luo, C., 2003. A less dusty future? Geophys. Res. Lett. 30 (17), 1903. http://dx.doi.org/10.1029/2003GL017880.

Mahowald, N.M., Yoshioka, M., Collins, W.D., et al., 2006. Climate response and radiative forcing from mineral aerosols during the last glacial maximum, pre-industrial, current and doubled-carbon dioxide climates. Geophys. Res. Lett. 33, L20705. http://dx.doi.org/10.1029/2006GL026126.

Marticorena, B., Bergametti, G., 1995. Modeling the atmospheric dust cycle: 1. Design of soil-derived dust emission scheme. J. Geophys. Res. 100 (D8), 16415−16430.

Mie, G., 1908. Beiträge zur optik trüber medien, speziell kolloidaler metallösungen. Ann. Phys. 25 (3), 377−445.

Nakicenovic, N., Alcamo, J., Davis, G., et al., 2000. Special Report on Emissions Scenarios: A Special Report of Working Group III of the Intergovernmental Panel on Climate Change. Cambridge University Press, Cambridge.

Pal, J.S., Small, E.E., Eltahir, E., 2000. Simulation of regional-scale water and energy budgets: representation of subgrid cloud and precipitation processes within RegCM. J. Geophys. Res. 105 (D24), 29579−29594.

Pal, J.S., Giorgi, F., Bi, X., et al., 2007. Regional climate modeling for the developing world: the ICTP RegCM3 and RegCNET. Bull. Am. Meteorol. Soc. 88 (9), 1395−1409.

Shao, Y., Dong, C., 2006. A review on East Asian dust storm climate, modelling and monitoring. Glob. Planet. Change 52, 1−22.

Shenk, W.E., Curian, R.J., 1974. The detection of dust storms over land and water with satellite visible and infrared measurements. Mon. Weather. Rev. 102, 820−837.

Please cite this article in press as: ZHANG, D.-F., et al., Effects of climate changes on dust aerosol over East Asia from RegCM3, Advances in Climate Change Research (2016), http://dx.doi.org/10.1016/j.accre.2016.07.001

Shi, G.-Y., Zhao, S.-X., 2003. Several scientific issues of studies on the dust storms. Chin. J. Atmos. Sci. 27 (4), 591−606 (in Chinese).

Shi, Y., 2010. A High Resolution Climate Change Simulation of the 21st Century over East Asia by RegCM3. Doctoral dissertation. Institute of Atmospheric Physics, Chinese Academy of Science (in Chinese).

Solmon, F., Giorgi, F., Liousse, C., 2006. Aerosol modeling for regional climate studies: application to anthropogenic particles and evaluation over a European/African domain. Tellus B 58 (1), 51−72.

Tegen, I., Werner, M., Harrison, S.P., et al., 2004. Relative importance of climate and land use in determining present and future global soil dust emission. Geophys. Res. Lett. 31, L05105. http://dx.doi.org/10.1029/2003GL019216.

USDA (U.S. Department of Agriculture), 1999. Soil Taxonomy: A Basic System of Soil Classification for Making and Interpreting Soil Surveys. U.S. Government Printing Office, Washington, U.S.

Westphal, D.L., Toon, O.B., Carlson, T.N., 1988. A case study of mobilization and transport of Saharan dust. J. Atmos. Sci. 45 (15), 2145−2175.

Xu, C.-H., 2010. Simulation and Project of Extremes Climate Events in China by Global Climate Models. Doctoral dissertation. Institute of Atmospheric Physics, Chinese Academy of Science (in Chinese).

Zakey, A.S., Solmon, F., Giorgi, F., 2006. Implementation and testing of a desert dust module in a regional climate model. Atmos. Chem. Phys. 6, 4687−4704.

Zhang, D.-F., Zakey, A.S., Gao, X.-J., et al., 2009. Simulation of dust aerosol and its regional feedbacks over East Asia using a regional climate model. Atmos. Chem. Phys. 9, 1095−1110.

Zhang, J., Christopher, S.A., 2003. Longwave radiative forcing of Saharan dust aerosols estimated from MODIS, MISR, and CERES observation on Terra. Geophys. Res. Lett. 30 (23), 2188. http://dx.doi.org/10.1029/2003GL018479.

Zhang, X.-Y., Arimoto, R., An, Z.-S., 1997. Dust emission from Chinese desert sources linked to variations in atmospheric circulation. J. Geophys. Res. 102, 28041−28047.

Zhou, Z.-J., Zhang, G.-C., 2003. Typical severe dust storms in northern China during 1954−2002. Chin. Sci. Bull. 48 (21), 2366−2370.

Please cite this article in press as: ZHANG, D.-F., et al., Effects of climate changes on dust aerosol over East Asia from RegCM3, Advances in Climate Change Research (2016), http://dx.doi.org/10.1016/j.accre.2016.07.001